Article

Cell Reports

Chaperone-Facilitated Aggregation of Thermo-Sensitive Proteins Shields Them from Degradation during Heat Stress

Graphical Abstract

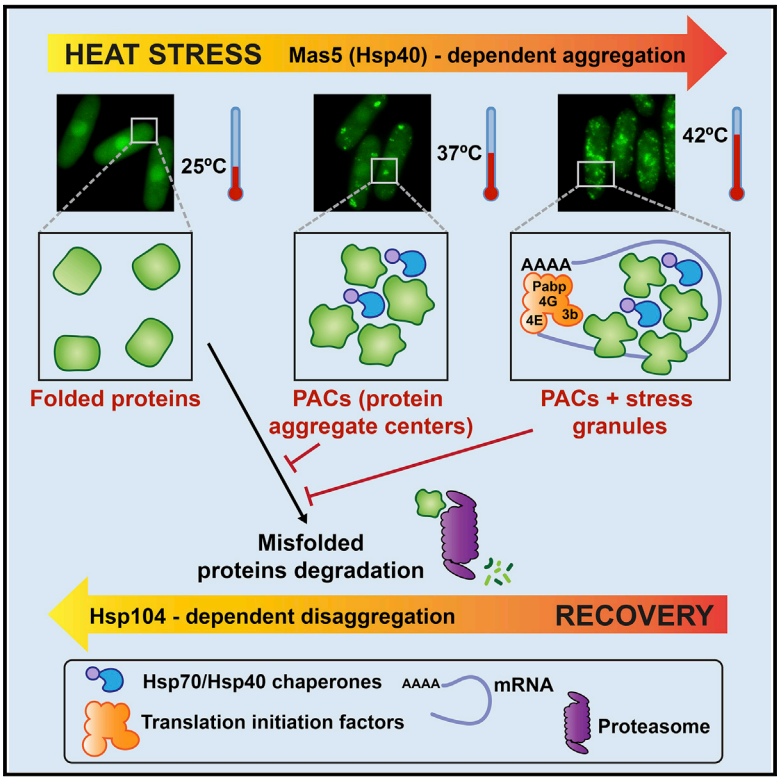

Highlights

- Misfolded proteins collapse into protein aggregate centers (PACs) upon heat shock
- PAC formation requires the Hsp40 chaperone Mas5
- PACs serve as seed for the nucleation of stress granules at severe temperatures
- The fate of PACs is refolding, as they protect misfolded proteins from degradation

Authors

Margarita Cabrera, Susanna Boronat, Luis Marte, Montserrat Vega, Pilar Pérez, José Ayté, Elena Hidalgo

Correspondence

margarita.cabrera@upf.edu (M.C.), elena.hidalgo@upf.edu (E.H.)

In Brief

The formation of aggregate foci upon heat shock is often considered a hallmark of toxicity. Cabrera et al. show that misfolded substrates are sequestered into protein aggregate centers (PACs) in a chaperone-mediated adaptation strategy. Proteins at PACs are protected from degradation, and they can refold after heat stress.

Cabrera et al., 2020, Cell Reports *30*, 2430–2443
February 18, 2020
https://doi.org/10.1016/j.celrep.2020.01.077

CellPress

OPEN ACCESS
CellPress

Cell Reports
Article

Chaperone-Facilitated Aggregation of Thermo-Sensitive Proteins Shields Them from Degradation during Heat Stress

Margarita Cabrera,[1,3,*] Susanna Boronat,[1,3] Luis Marte,[1] Montserrat Vega,[1] Pilar Pérez,[2] José Ayté,[1] and Elena Hidalgo[1,4,*]

[1]Oxidative Stress and Cell Cycle Group, Universitat Pompeu Fabra, C/ Dr. Aiguader 88, 08003 Barcelona, Spain
[2]Instituto de Biología Funcional y Genómica (IBFG), Consejo Superior de Investigaciones Científicas, University of Salamanca, 37007 Salamanca, Spain
[3]These authors contributed equally
[4]Lead Contact
*Correspondence: margarita.cabrera@upf.edu (M.C.), elena.hidalgo@upf.edu (E.H.)
https://doi.org/10.1016/j.celrep.2020.01.077

SUMMARY

Cells have developed protein quality-control strategies to manage the accumulation of misfolded substrates during heat stress. Using a soluble reporter of misfolding in fission yeast, Rho1.C17R-GFP, we demonstrate that upon mild heat shock, the reporter collapses in protein aggregate centers (PACs). They contain and/or require several chaperones, such as Hsp104, Hsp16, and the Hsp40/70 couple Mas5/Ssa2. Stress granules do not assemble at mild temperatures and, therefore, are not required for PAC formation; on the contrary, PACs may serve as nucleation centers for the assembly of stress granules. In contrast to the general belief, the dominant fate of these PACs is not degradation, and the aggregated reporter can be disassembled by chaperones and recovers native structure and activity. Using mass spectrometry, we show that thermo-unstable endogenous proteins form PACs as well. In conclusion, formation of PACs during heat shock is a chaperone-mediated adaptation strategy.

INTRODUCTION

Proteins must fold into their unique native structures to be functional, and the process of synthesis is tightly regulated to ensure efficient processing (for reviews, see Gloge et al., 2014; Pechmann et al., 2013). Once they are synthesized, the structure of native proteins is not rigid, and a network of chaperones and degradation machineries maintain the integrity of the proteome, constituting the protein quality-control (PQC) system meant to recognize, refold, and degrade aberrant proteins to maintain protein homeostasis, also known as proteostasis (for reviews, see Balchin et al., 2016; Kim et al., 2013; Pilla et al., 2017).

Heat shock alters proteostasis so that the PQC system is challenged. Thus, when heat alters the equilibrium between protein synthesis, folding, and degradation, the cell has to activate signaling events, often driven and/or executed by chaperones, to avoid accumulation of misfolded proteins and decide their fate toward folding or degradation. The heat-shock-induced cell response includes upregulation of chaperones, which try to reverse the effects of the stress by refolding non-native protein conformations, and also of clearance functions, such as autophagy and the ubiquitin-proteasome system (UPS) (for reviews, see Dikic, 2017 and Kleiger and Mayor, 2014).

Following non-lethal heat shock, both newly synthesized and mature, fully functional proteins misfold and can, eventually, accumulate into aggregation-like structures of different physical properties and subcellular localizations. Because the hallmarks of many neurodegenerative disorders are aggregates of misfolded proteins (such as huntingtin in Huntington disease or beta-amyloid in Alzheimer disease), the presence of protein aggregates in cells has often been linked to toxicity, so that preventing aggregate formation and accumulation is still proposed to be a priority goal of the PQC system. However, recent evidence demonstrating active and regulated deposition of misfolded polypeptides into specialized cellular locations challenges the view that links aggregation and toxicity.

Thus, an important part of PQC is the local management of misfolded proteins into specific subcellular compartments. The exact functions of each of these PQC compartments are still to be discovered, although mainly two fates have been proposed: to enhance aggregated protein clearance by the degradation machineries or to sequester otherwise toxic prion-like molecules into safe, isolated areas away from the functional proteome. Thus, the *Saccharomyces cerevisiae* Q-bodies are formed early upon heat-shock-induced misfolding, and they are then cleared through the UPS; if degradation is impaired, Q-bodies mature into juxtanuclear quality-control compartments (JUNQ) (Escusa-Toret et al., 2013; Kaganovich et al., 2008). The insoluble protein deposits (IPODs) in yeast, equivalent to the perinuclear aggresome in mammalian cells, exemplify the second proposed function: a site of terminal sequestration of toxic molecules (Kaganovich et al., 2008) (for a recent review, see Sontag et al., 2017). In this line, formation of aggregate-like centers would be a regulated phenomenon to promote healthy aging by sequestering old, aged proteins that expose hydrophobic domains (Erjavec et al., 2007; Zhou et al., 2014).

In recent years, a new function has emerged for the coalescence of proteins into intracellular bodies: chaperone-mediated refolding of aggregated proteins during stress recovery, with Hsp104 exerting an essential role (Cherkasov et al., 2013; Glover and Lindquist, 1998); this disaggregation could be performed from the aggregate centers (for a recent review, see Nillegoda et al., 2018). Indeed, it has been recently described again in budding yeast that heat-shock-dependent aggregate formation is a reversible process so that the activity of proteins can be regained as an adaptation strategy to facilitate growth resumption (Wallace et al., 2015). Nevertheless, the formation of these regulated aggregate-like centers has been described at extreme temperatures, namely, 46°C, which is very close to lethality.

Here, we have analyzed the impact of mild heat shock on the PQC system in fission yeast by monitoring the behavior of a new fluorescent reporter protein with dual cytosolic and nuclear localization, Rho1.C17R-GFP. Even at very mild temperatures, such as 37°C, this and other soluble reporters form reversible aggregate-like structures, which we have termed protein aggregate centers (PACs). Evidence suggests that the formation of these PACs is an adaptation strategy central to the PQC system: (1) it is driven and/or accompanied by several heat shock proteins (HSPs); (2) two classical markers of aggregation, Hsp104-GFP and Hsp16-GFP, also coalesce into PACs in cells that do not express the reporter Rho1.C17R-GFP, suggesting that endogenous proteins also form PACs; (3) formation of stress granules (SGs) upon severe heat shock may be facilitated by the assembly of PACs; and (4) the physiological role of PAC formation is to shield misfolded proteins from degradation until conditions allow disaggregation of non-terminally misfolded proteins by molecular chaperones. Furthermore, we have isolated and identified by mass spectrometry (MS) the fraction of thermally sensitive fission yeast proteins, which only assemble into PACs upon heat stress. We propose that PAC formation in fission yeast is an organized process that prevents degradation of misfolded proteins until temperature conditions allow their disaggregation into native, functional proteins to promote cell fitness and growth resumption.

RESULTS

Rho1.C17R-GFP Forms PACs upon Mild Temperature Up-Shift

To study cytosolic PQC in *Schizosaccharomyces pombe,* we searched for thermo-sensitive mutant proteins that could misfold upon heat shock. Rho1 is an essential small GTPase regulating cell wall biosynthesis, actin organization, and polarized growth (Park and Bi, 2007; Pérez and Cansado, 2010). Most GTPases of the Ras and Rho families undergo lipid modifications at their C-terminal domains for proper targeting to cell membranes. In particular, Rho1 undergoes geranylgeranylation at Cys199, and this protein modification promotes Rho1 localization at the plasma membrane (Sánchez-Mir et al., 2014). The Rho1 thermo-sensitive mutant Rho1-596 carries a missense mutation causing a Cys17-to-Arg substitution in the GTP-binding domain; Rho1.C17R almost disappeared from cell extracts upon mild heat shock (Viana et al., 2013). We constitutively expressed GFP-Rho1 and GFP-Rho1.C17R in wild-type cells from an integrative plasmid (Figure 1A, membrane-anchored Rho1), and both proteins display plasma membrane localization at a permissive temperature (25°C, Figure 1B). As previously described, the GFP fluorescence of cells expressing GFP-Rho1.C17R (but not that of GFP-Rho1-expressing cells) vanishes after 2 h of incubation at 37°C (Figure 1B).

We then engineered non-membrane-associated Rho1.C17R derivatives by either eliminating the lipidation target residue Cys199 or by fusing GFP or mCherry to the C-terminal domain of Rho1, expecting that the tag would hinder Cys199 from geranylgeranyl transferases (Figure 1A, cytosolic/nuclear Rho1). As shown in Figures 1C and S1A, the prenylation-defective mutants Rho1.C17R-GFP, GFP-Rho1.C17R.C199S, and Rho1.C17R-mCherry displayed dual cytosolic and nuclear localization at the permissive temperature. Upon mild heat shock, the three reporters form foci, 2–4 per cell. As an indicator of protein misfolding, we compared the solubility of cytosolic Rho1.C17R-GFP at permissive (25°C) and restrictive (37°C) temperatures: the reporter was found predominantly in the soluble form at 25°C (S in Figure 1D), whereas 1 h after incubation at 37°C the protein was highly enriched in the NP-40-insoluble fraction (P in Figure 1D). These data suggest that Rho1.C17R-GFP is a good temperature-sensitive reporter, non-bound to membranes, which forms detergent-insoluble aggregates upon mild heat shock. It is worth mentioning that a shift to 37°C is a moderate heat shock for fission yeast, which does not slow growth nor exerts toxicity to wild-type cultures, but significantly affects the viability of cells lacking stress signaling components, such as the MAP kinase Sty1 (Figures 1E and S1B).

We analyzed the kinetics of foci formation upon heat shock at 37°C and 42°C; at the higher temperature, growth of wild-type cells is permanently halted, both in liquid and solid media (Figures 1E and S1B), translation is fully inhibited (Humphrey and Enoch, 1998), and viability is compromised (Figure S1C). Again, the localization of Rho1.C17R-GFP after a shift to 37°C changes from its homogeneous cytosolic/nuclear distribution to the appearance of foci at 30 min, which is maximal at 60 min, with 2–4 aggregate-like centers in nearly all cells (Figure 1F). Upon a shift to 42°C, foci formation is much faster and multiple centers, 10–20 per cell, are present in all cells in both the cytosol and the nucleus. From now on, we will call these foci PACs. The number, timing, and appearance of these PACs vary depending on the temperature applied.

Several Chaperones, Such as Hsp104, Hsp16, Hsp90 Swo1, Hsp70s Ssa1 and Ssa2, and Hsp40s Psi1 and Mas5, Are Present at PACs

Once we determined that our thermo-sensitive reporters form PACs upon mild heat shock, we analyzed the composition of PACs regarding proteins of the PQC system. Thus, we first monitored the localization of the disaggregase Hsp104, which is reported to associate with aggregated proteins in different biological systems (for a review, see Mogk et al., 2015). A GFP-tagged Hsp104 retaining functionality was selected (Figure S1D), and will be used hereafter. The simultaneous expression of Rho1.C17R-mCherry and Hsp104-GFP in cells revealed an almost complete overlap or co-localization upon heat stress (Figures 2A and S1E), which indicates that Hsp104 and temperature-sensitive mutants share the same fate and are confined into the same spatial localizations, the PACs.

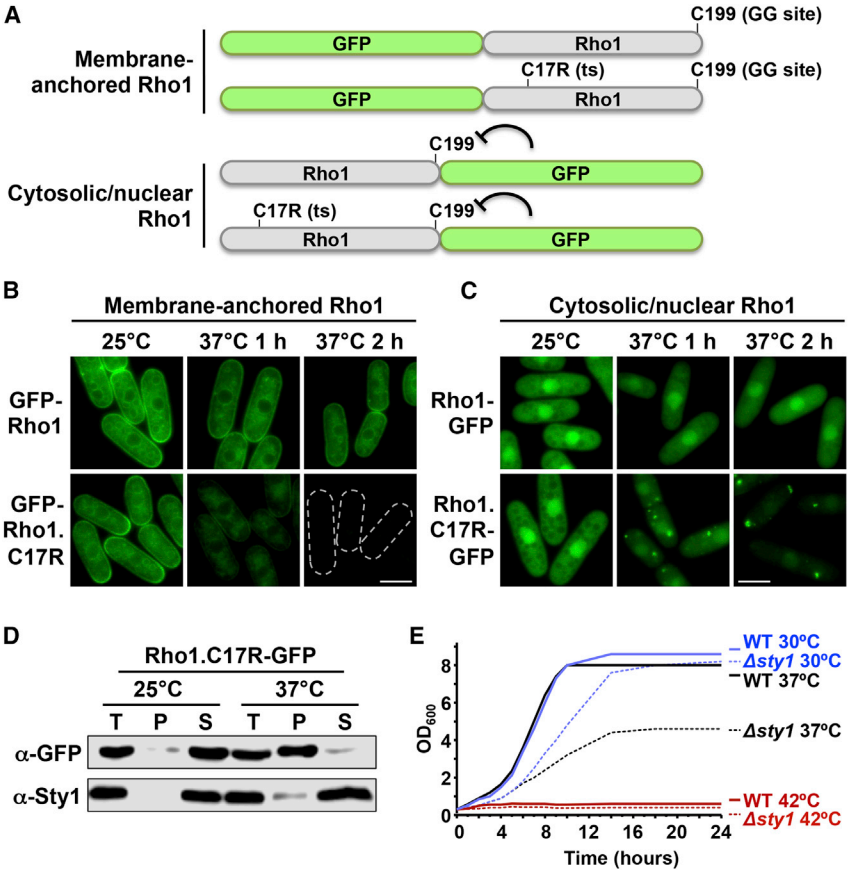

Figure 1. A Temperature-Sensitive Mutant of Rho1 Accumulates at PACs

(A) Scheme depicting the different versions of Rho1 used in this study. C17R, temperature-sensitive mutation of Cys17-to-Arg; C199, geranylgeranylation site (GG), which access is prevented by C-terminal tagging of Rho1 with GFP.

(B and C) The cytosolic/nuclear versions of Rho1 mutant concentrate at PACs upon heat shock. Cells expressing membrane-anchored (B) or cytosolic/nuclear variants (C) of Rho1 WT and C17R mutant were analyzed by fluorescence microscopy upon heat shock at 37°C for 1 or 2 h.

(D) Rho1.C17R is enriched in the insoluble fraction after heat shock. Solubility of Rho1.C17R-GFP after heat shock at 37°C for 1 h was examined by subcellular fractionation and immunoblotting using anti-GFP antibody and anti-Sty1 as loading control (T, total; P, pellet fraction; S, soluble fraction).

(E) Growth at 37°C only reduces viability in cells with defective stress response. OD_{600} of cell cultures of WT and *Δsty1* strains at the indicated temperatures was measured using a spectrophotometer. This is one of three experiments with very similar growth profiles.

(F) Severe heat shock induces a very rapid assembly of PACs. Formation of protein foci was monitored by fluorescence microscopy in cells expressing Rho1.C17R-GFP at the indicated time points and heat shock conditions. Maximum-intensity projections of z stacks (6 planes, 0.4-μm steps) are shown.

Scale bars, 5 μm. See also Figure S1.

We tagged different proteins of the PQC and of the ribosome quality-control systems with GFP and co-expressed them with our cytosolic/nuclear misfolding reporter Rho1.C17R-mCherry. We chose members of the Hsp70, Hsp40, and Hsp90 families and large/small HSPs. We unambiguously found co-localization at PACs at both 37°C (Figure 2A) and 42°C (Figure S1E) of our thermo-sensitive reporter and Hsp16, the Hsp70s Ssa1 and Ssa2, the Hsp90 Swo1, and the Hsp40s Psi1 and Mas5. The PQC components Sks2 (ribosome-associated Hsp70), Scj1 (Hsp40 linked to the endoplasmic reticulum), Bag102 (BAG-family member linked to the proteasome), and Ssz1 and Zuo1 (components of the ribosome-associated complex [RAC]) are not present in the foci (Figure S1F).

The Hsp40/70 Chaperones Mas5/Ssa2 Are Required for PAC Assembly

The formation of PACs at very mild temperatures and the presence of several chaperones at these centers raise the question of whether some PQC components may be involved in the decision to assemble the PACs. With the idea that some chaperones may be required to recognize misfolded structures and sort them toward formation of these compartmentalized centers, we expressed Rho1.C17R-GFP in cells lacking specific chaperones. As shown in Figure S2A, the lack of Hsp16, Bag102 (proteasome component), Ssa1 (Hsp70), Hul5 or San1 (E3 ubiquitin ligases), or Btf3 or Egd2 (components of the nascent polypeptide-associated complex [NAC]) had no effect on the formation of PACs at either 37°C or 42°C. On the contrary, the absence of Scj1, Ssz1 or Zuo1, Psi1 (Hsp40), Hsp104 or Sks2 had a small but significant negative influence on the formation of these centers at 37°C, but not at 42°C (Figures 2B and S2B–S2D). Importantly, PACs were absent in 100% of *Δmas5* cells at both temperatures (Figure 2B). As can be observed in the fluorescence images (Figure 2B) and by western blot (Figure S3A), the concentration of our reporter, Rho1.C17R-GFP, in cells lacking Mas5 is significantly lower than in wild-type cells, suggesting a role of this Hsp40 chaperone in protein folding in the absence of heat stress. To dismiss an effect due to protein concentrations, we expressed our reporter under the control of the weaker *nmt41* promoter, which yielded protein levels in wild-type cells equivalent to those accomplished using the *sty1* promoter in *Δmas5* (Figure S3B). Even at these low levels, Rho1.C17R-GFP formed PACs in wild-type cells upon

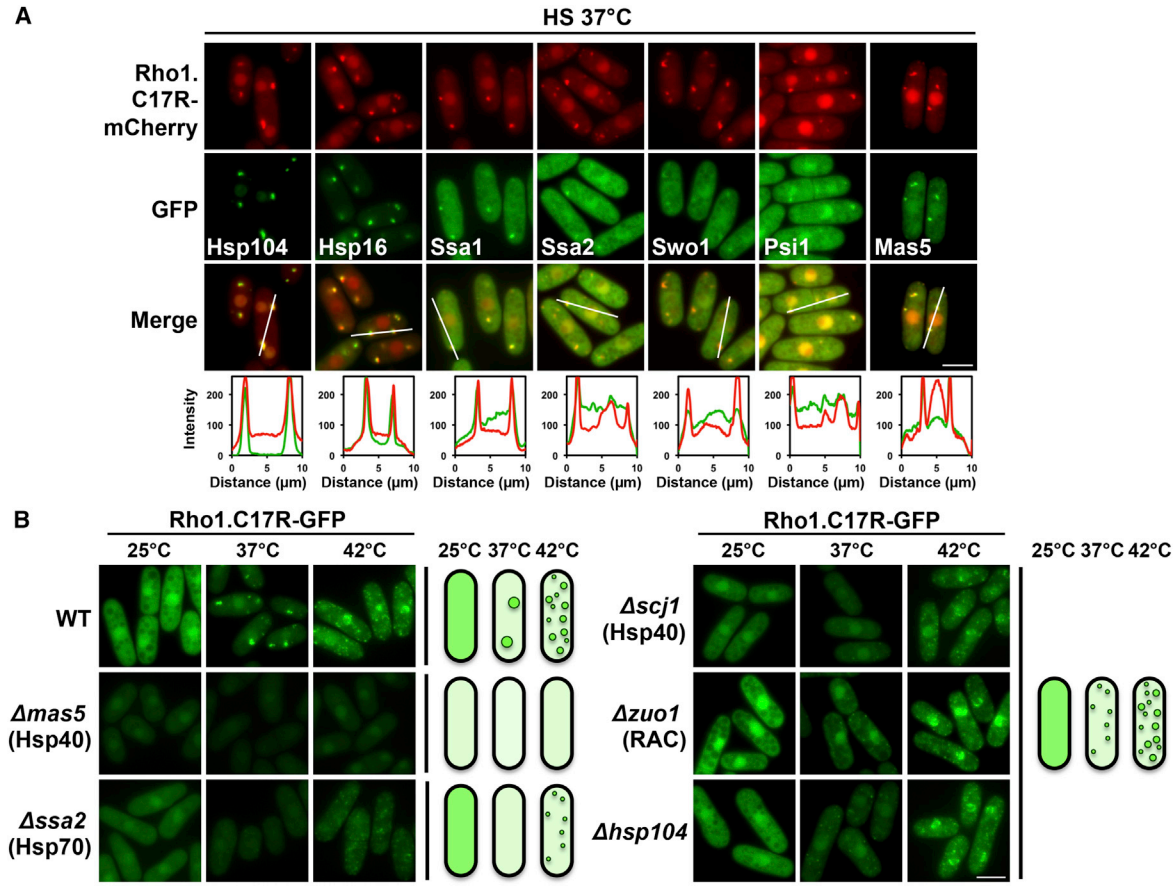

Figure 2. Identification of Chaperones Required for Heat-Shock-Induced PAC Assembly

(A) Co-localization analysis of Rho1.C17R-mCherry with different GFP-tagged chaperones in strains grown at 25°C and incubated at 37°C for 1 h. Line intensity plots of Rho1.C17R-mCherry and GFP-tagged chaperones are shown.

(B) Formation of PACs labeled with Rho1.C17R-GFP was analyzed by fluorescence microscopy in the indicated deletion strains after incubation at 37°C for 1 h or 42°C for 15 min.

Scale bars, 5 μm. See also Figures S1–S3.

heat shock (Figure S3C). Mas5 is an Hsp40 chaperone known to associate with the Hsp70 protein Ssa2 (Vjestica et al., 2013). The lack of Ssa2 also significantly impaired PAC formation (Figure 2B), although to a lesser extent that the lack of Mas5, probably due to certain functional redundancy with other Hsp70s such as Ssa1.

PACs Provide a Platform for Building SGs under Severe Heat Stress

During heat and other stresses, SGs are transient storage sites for ribosome-free mRNAs and proteins involved in translation initiation, such as eIF4G, eIF4E, eIF4B, eIF4A, and poly(A) binding protein, for their later use upon growth resumption. The presence of chaperones and misfolding reporters at SGs in different model systems (Cherkasov et al., 2013; Kroschwald et al., 2015) suggests a putative coordination in the origin of these mRNA stress control compartments and those of aggregated protein centers, as parallel strategies to cope with stress. Little is known about the formation and composition of SGs in fission yeast; it has been described that various stimuli, including heat shock, glucose deprivation, arsenite, or osmotic stresses can trigger SG formation (Nilsson and Sunnerhagen, 2011; Satoh et al., 2012; Wang et al., 2012; Wen et al., 2010).

We tagged several translation initiation factors with GFP in wild-type cells and tested their localization upon mild and severe heat shock. To monitor SG formation, we directly shifted logarithmic cell cultures (optical density 600 [OD_{600}] of 0.5) to the indicated temperatures, as done before to detect PAC formation, or concentrated them by centrifugation prior to heat shock application, as reported before by other groups (Satoh et al., 2012; Wen et al., 2010). As shown in Figures 3A and S4A, GFP-tagged eIF4E, eIF4G, poly(A) binding protein Pabp, eIF3b, and eIF4B display cytosolic localization at both 25°C and 37°C; this temperature up-shift is sufficient to trigger PAC formation but not to detect SGs. The translation inhibitor puromycin (PUR) has been described to facilitate SG formation in other model systems (Bounedjah et al., 2014; Kedersha et al., 2000; Mollet et al., 2008), but it does not promote SG deposition at 37°C (Figure S4B). All the translation initiation reporters, except eIF4B (Figure S4A), form foci at 42°C and/or 46°C, with eIF4E being

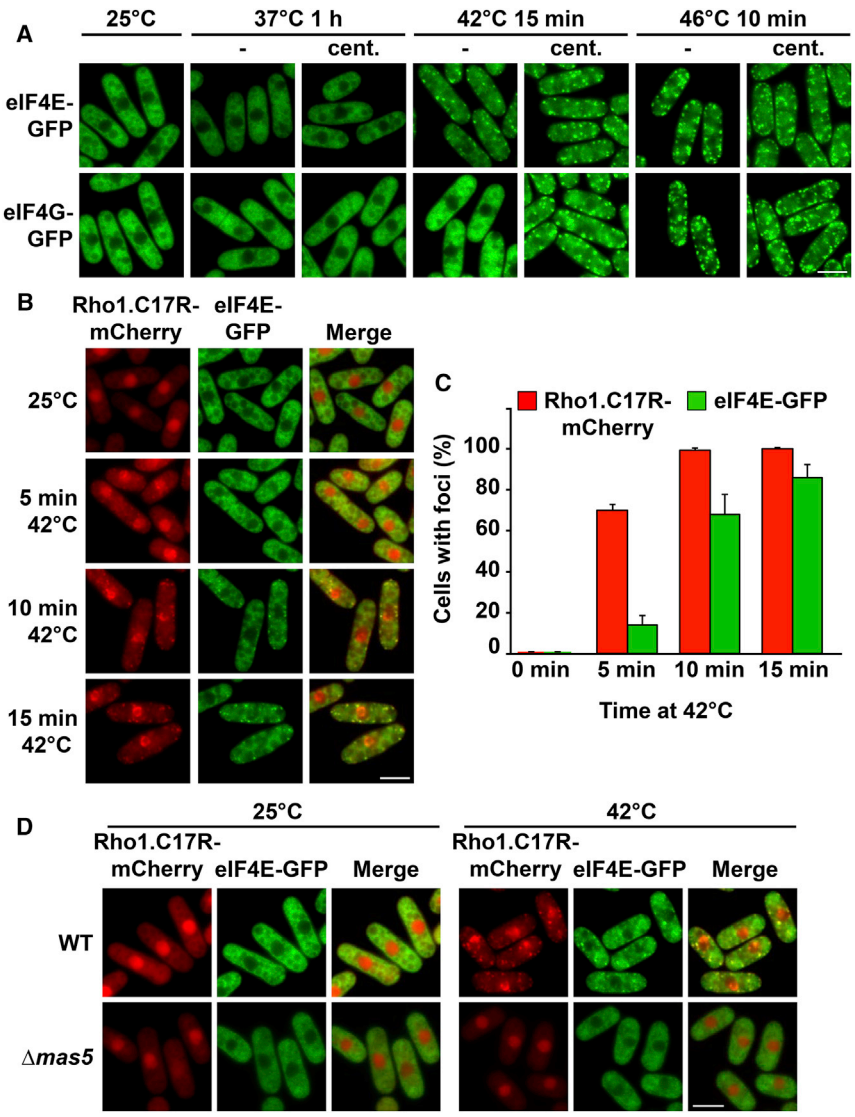

Figure 3. PACs Serve as a Platform for Stress Granule Assembly

(A) Stress granules are visible after heat shock at 42°C and 46°C but not at 37°C. C-terminally GFP-tagged translation initiation factors eIF4E and eIF4G were used as stress granule markers. Where indicated, cells were concentrated by centrifugation (cent.) before heat shock treatment.

(B) At 42°C, PACs labeled with Rho1.C17R appear earlier than stress granules, as monitored in cells co-expressing Rho1.C17R-mCherry and eIF4E-GFP after incubation at 42°C for the indicated times.

(C) Percentage of cells from (B) containing Rho1.C17R-mCherry or eIF4E-GFP-positive foci ($n > 100$). Values represent the mean + SEM of three independent experiments.

(D) Lack of Mas5 abolishes both PAC formation and the assembly of stress granules. We applied heat shock at 42°C for 15 min in WT and *Δmas5* cells co-expressing Rho1.C17R-mCherry and eIF4E-GFP. Scale bars, 5 μm. See also Figure S4.

the only one forming SGs at 42°C in the absence of prior centrifugation (Figure 3A). As described before for SGs, some ribosomal proteins do not collapse into these foci (Figure S4C). We conclude that SGs are formed in fission yeast at temperatures much higher than those required to detect PAC formation, therefore demonstrating that they are different entities.

To monitor whether PACs and SGs co-localize upon severe heat shock, we co-expressed eIF4E-GFP and Rho1.C17R-mCherry. Co-localization between both protein markers is complete at 46°C at all times (Figure S4D). However, when cultures were shifted to 42°C, PAC formation clearly preceded SG formation (Figures 3B and 3C), suggesting that PACs, which are also observed at mild temperatures that do not favor SG coalescence, serve as seeds for the assembly of SGs at high, toxic temperatures. Indeed, a lack of Mas5, which completely impairs PAC formation (see Figure 2B), also compromises the assembly of SGs (Figure 3D), even at extreme temperatures (Figure S4E). Thus, non-native misfolded proteins constitute a platform for the deposition of translation initiation factors and, likely, ribosome-naked mRNAs to form SGs, at least in response to heat shock.

PAC Assembly Shields Misfolded Proteins from Proteasomal Degradation

It has been proposed by the group of Li that heat-induced aggregation is blocked by the translation elongation inhibitor cycloheximide (CHX) and, thus, that aggregate formation requires active translation (Zhou et al., 2014). By contrast, the group of Tamás reported that CHX cannot block the formation of Hsp104-containing foci after heat shock (Jacobson et al., 2012). To investigate the contribution of new protein synthesis on heat-dependent PAC assembly, we treated cells with CHX during heat shock imposition. As shown in Figure 4A, the formation of PACs at 37°C is fully abolished by treatment with CHX, whereas PAC assembly at 42°C is only partially inhibited (Figure S5A). The same occurs upon treatment with the translation inhibitor anisomycin (Figure S5B). However, protein synthesis inhibition per se is not the cause of this blockage on PAC assembly: the translation inhibitor PUR fails to inhibit, and even favors, formation of PACs (Figure 4A). Although CHX and anisomycin inhibit translation elongation and freeze ribosomes (and, probably, premature polypeptides) on translating mRNAs, PUR destabilizes polysomes by promoting premature termination, probably releasing from mRNAs not only ribosomes and ribosome-associated PQC components but also non-fully folded premature polypeptides (Figure 4B). These results suggest that defective translation products, which occur upon heat shock imposition in normal untreated cells or chaperones linked to *de novo* protein synthesis, may significantly contribute to PAC assembly in fission yeast,

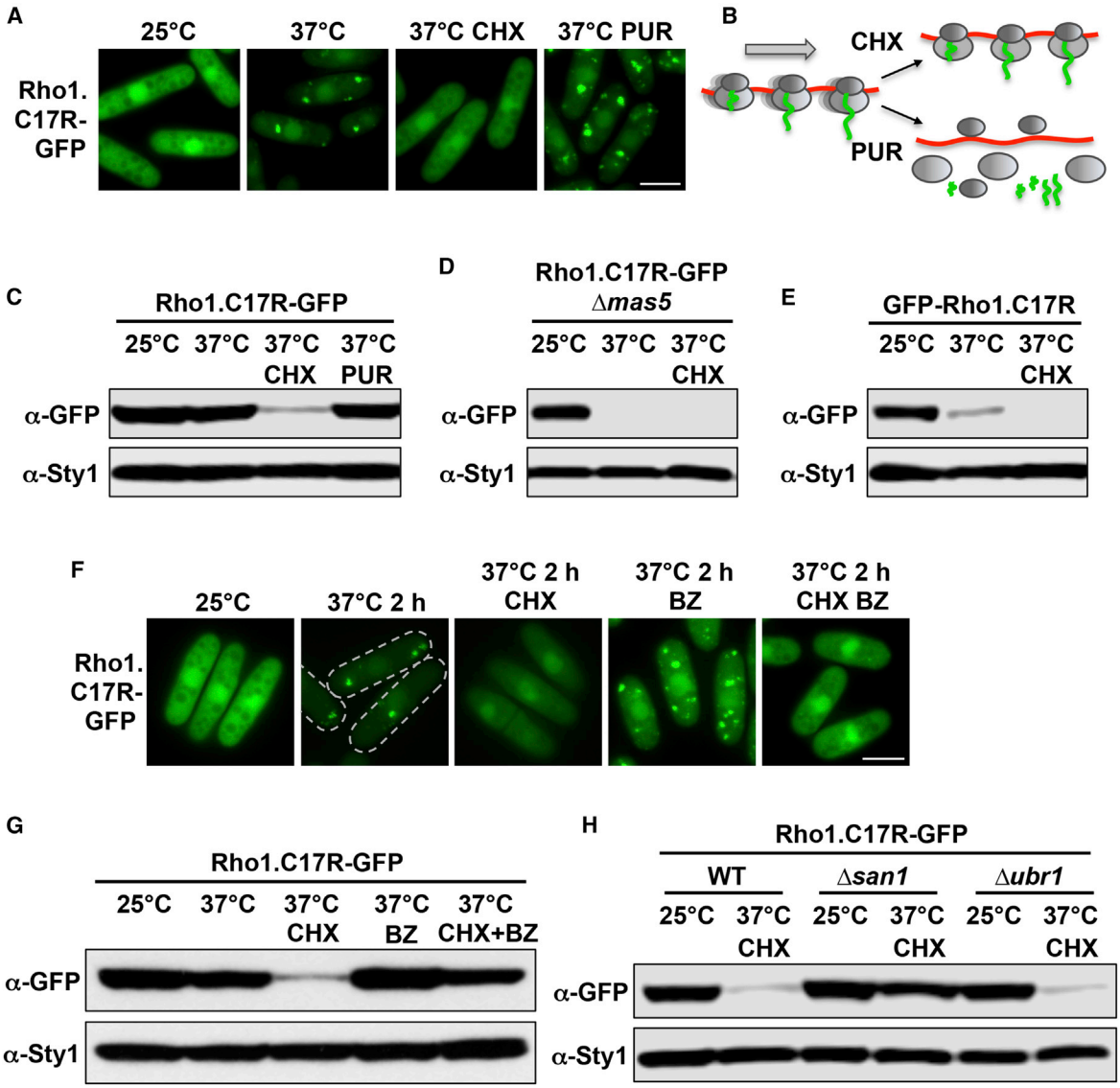

Figure 4. PAC Assembly Prevails upon Heat Shock Treatment and Avoids Protein Degradation

(A) CHX, but not PUR, prevents PAC assembly. Formation of PACs labeled with Rho1.C17R-GFP was examined after incubation at 37°C for 1 h. Where indicated, cells were treated with CHX (100 μg/ml) or PUR (1 mM) to inhibit translation.

(B) Scheme depicting the different effects in translation of CHX (which "freezes" the ribosomes on the translated mRNAs) and PUR (which causes premature translation termination).

(C) Heat-shock-induced Rho1.C17R-GFP degradation only occurs upon CHX, but not PUR, treatment. Cells expressing Rho1.C17R-GFP were incubated at 37°C for 2 h with CHX or PUR, trichloroacetic acid (TCA) extracts were obtained, and protein levels detected by immunoblotting using anti-GFP antibody; anti-Sty1 was used as a loading control.

(D) Rho1.C17R-GFP degradation was induced by heat shock at 37°C in cells lacking Mas5, where PAC assembly is blocked. Experiment was performed as in (C).

(E) Heat-shock-induced degradation of the membrane-anchored GFP-Rho1.C17R occurs even in the absence of CHX. Experiment was performed as in (C).

(F) Heat-shock- and CHX-dependent degradation of Rho1.C17R-GFP is blocked upon proteasome inhibition. Fluorescence microscopy of cells expressing Rho1.C17R-GFP after heat shock at 37°C for 2 h, in the presence or not of CHX and the proteasome inhibitor bortezomib (BZ, 0.1 mM). Dashed lines indicate the borders of yeast cells.

(G) Rho1.C17R-GFP protein levels were detected in TCA extracts from cells treated as in (F). Experiment was performed as in (C).

(H) The E3 ligase San1 is required for the proteasomal degradation of Rho1.C17R.GFP in the presence of CHX. Cell cultures of the indicated strains were treated as in (F), and protein detection was made as in (C).

Fluorescence images represent maximum-intensity projections of z stacks (9 planes, 0.3-μm steps). Scale bars, 5 μm. See also Figure S5.

and translation inhibitors that freeze polysomes (such as CHX or anisomycin) abolish PAC seeding arising from active translation.

Taking advantage of the different effects of translation inhibitors on PAC assembly, we analyzed whether the accumulation of misfolded proteins into foci, which is prevented by CHX

treatment but not by PUR, has any effect on the turnover of misfolded proteins. The concentration of Rho1.C17R-GFP is not significantly affected by heat shock at 37°C, even when protein synthesis is blocked by PUR. However, in the presence of CHX, which not only avoids *de novo* Rho1.C17R-GFP synthesis but also inhibits PAC assembly, the protein is degraded after 2 h of incubation at 37°C (Figure 4C). These data suggest that interventions blocking PAC formation, such as CHX co-treatment, favor degradation of misfolded substrates.

We tested this hypothesis by analyzing the stability of Rho1.C17R-GFP in cells lacking Mas5, in which PAC formation is fully blocked (Figure 2B). In this strain background, the protein fully disappears from extracts upon heat shock, in the presence or absence of CHX (Figure 4D) or PUR (Figure S5C).

A third example of experimental evidence suggesting that PACs shield misfolded proteins from degradation comes from the analysis of the membrane-anchored GFP-Rho1.C17R, which does not coalesce into foci upon heat imposition (Figure 1B). As shown in Figure 4E and as reported before (Viana et al., 2013), the protein is degraded upon heat shock even without CHX.

The UPS is responsible for the clearance of most misfolded proteins (Amm et al., 2014). As shown in Figures 4F and 4G, the degradation of the reporter Rho1.C17R-GFP that occurs at 37°C when PAC formation is inhibited with CHX is fully abolished by the addition of the proteasome inhibitor bortezomib (BZ). Indeed, BZ can block the degradation of the reporter expressed in cells lacking Mas5 (Figure S5C). We tested the role of some E3 ubiquitin ligases that have been reported to participate in the degradation of specific protein clients in *S. pombe*, such as Ubr1 (Penney et al., 2012; Takeda and Yanagida, 2005), Ubr11 (Kriegenburg et al., 2014), Ltn1 (Mathiassen et al., 2015), Hul5, Pub1 or Pib1 (Kampmeyer et al., 2017), or San1 (Kriegenburg et al., 2014; Matsuo et al., 2011). Only the absence of San1 blocks degradation of the reporter (Figures 4H and S5D). This E3 ligase does not, however, participate in the degradation of the membrane-anchored reporter GFP-Rho1.C17R (Figure S5E).

We conclude that chaperone-facilitated aggregation of cytosolic/nuclear misfolded clients prevents their proteasomal degradation, which depends on the E3 ubiquitin ligase San1.

Proteins at PACs Are Not Destined for Degradation But for Refolding during Recovery

The data we have presented here suggest that PAC formation is a regulated process, and we hypothesized that the goal of this PQC strategy could be to maintain non-terminally misfolded proteins in a reversible stage, for future dissagregation/refolding during recovery at non-stressful temperatures. We have tracked the fate of Rho1.C17R-GFP at PACs during stress recovery, by shifting cultures from 37°C or 42°C to 25°C in the presence of CHX, to dismiss the effects of new protein synthesis. As shown by fluorescence microscopy, PACs assembled upon 37°C heat shock disappeared 2–3 h after the cultures were shifted back to permissive temperature, whereas absorption of the foci was even faster (1–2 h) from PACs assembled at 42°C (Figures 5A and 5C). Importantly, 42°C-assembled PACs require the presence of the disaggregase Hsp104 for disassembly, although the chaperone seems to be only partially required when PACs are assembled at 37°C (Figures 5A and 5C). This suggests that PACs assembled at 42°C, which do include SGs components (Figure 3B), fully depend on Hsp104 for disassembly. Yet, it remained unclear whether non-terminal misfolded proteins are back into their soluble, native, and active forms.

Thus, we tested whether the native protein structure of Rho1.C17R-GFP, suggestive of protein function recovery, was restored after heat shock cessation. As explained above, Rho1 is a GTPase, the GTP-bound form being the active protein, and the C17R mutation lies within the GTP-binding domain (Viana et al., 2013). Even though non-membrane-anchored GTPases are supposed to lack GTP, overexpression of Rho1.G15V.C199S, a constitutive active form that is not attached to the membrane, causes toxicity to wild-type cells (Arellano et al., 1998). This finding suggests that the GTPase can retain GTP binding capacity even when it is not anchored to the membrane. Therefore, we tested whether the amount of GTP-bound Rho1.C17R-GFP, as an indicator of active protein, could diminish upon heat shock and be restored after stress cessation. We prepared native extracts of cells expressing the reporter, and the GTP-bound Rho1 was pulled down from extracts with recombinant GST-C21RBD (Rhotekin Rho-binding domain; see STAR Methods) (Coll et al., 2003). The total amount of Rho1.C17R-GFP from whole-cell extracts, as determined by western blot using an anti-GFP antibody, does not vary patently. However, active GTP-bound protein from extracts of cells grown at 25°C fully disappears from extracts of cells grown at 37°C or 42°C (Figure 5D). The levels of active Rho1.C17R-GFP are fully restored 2 h after recovery at 25°C in the presence of CHX (Figure 5D), which indicates that the proteins at PACs are not terminally misfolded nor are destined to degradation but can rather regain native conformation and wild-type activity. This disaggregation capacity partially (37°C) or fully (42°C) depends on the Hsp104 disaggregase (Figure 5D).

Endogenous Proteins Also Assemble into PACs to Escape from Degradation

Rho1.C17R-GFP is an artificial reporter constitutively expressed from a heterologous promoter, which misfolds due to the Cys-to-Arg mutation. The behavior of the other designed probes, GFP-Rho1.C17R.C199S and Rho1.C17R-mCherry, was identical to that of Rho.C17R-GFP (Figure S1A; data not shown). To monitor whether PAC formation is a general strategy, not specific for the Rho1-derived reporters, to prevent misfolded protein degradation, we have pursued three types of strategies: (1) analyzed the fate of other thermo-sensitive reporters; (2) studied the heat-shock-dependent distribution of endogenous Hsp16-GFP, expressed in wild-type cells in the absence of any thermo-sensitive reporter; and (3) isolated the thermo-unstable *S. pombe* proteome and analyzed it by MS.

To visualize other misfolded clients that may follow the chaperone-mediated PAC assembly process described for Rho1.C17R-GFP, we monitored the behavior of two other non-membrane-bound reporters of misfolding: Ura4.L261P-GFP and Guk1-9-GFP. The temperature-sensitive Ura4.L261P, isolated by the group of Davey, supports growth at 30°C but not at 37°C in media lacking uracil (Davis et al., 1999). We substituted the endogenous *ura4* allele with the mutant *ura4.L261P* and tagged it with *GFP*. The *S. cerevisiae GUK1-9* allele, isolated by the group of

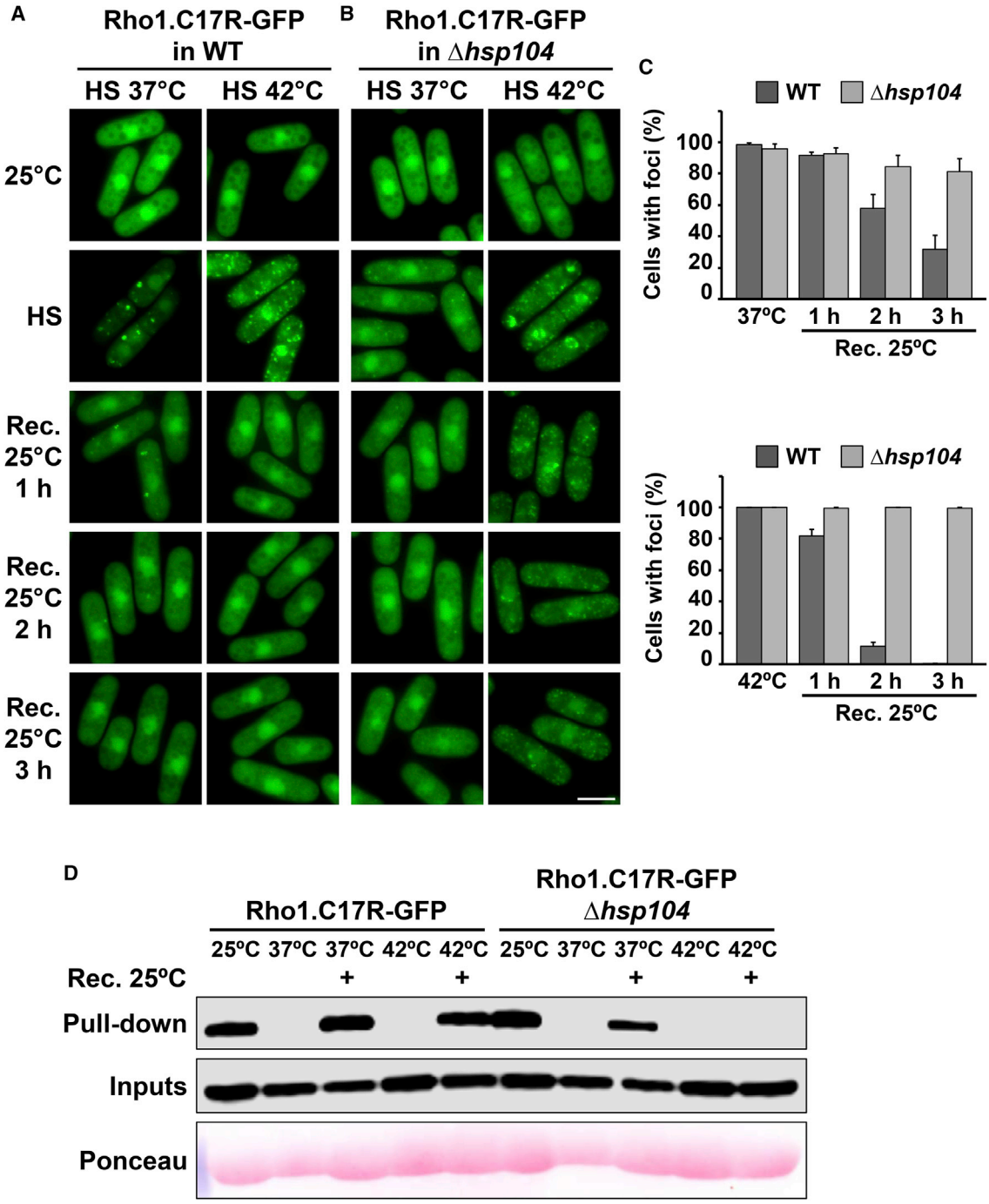

Figure 5. Protein Refolding Occurs after Hsp104-Dependent Disassembly of PACs

(A and B) Assembled PACs at 37°C or 42°C are dissolved during recovery at permissive temperature in an Hsp104-dependent manner. WT (A) or *Δhsp104* (B) cells expressing Rho1.C17R-GFP were heat-shocked at 37°C for 1 h or 42°C for 15 min and then incubated at 25°C in the presence of CHX to avoid new protein synthesis. Disaggregation of PACs was monitored at the indicated time points by fluorescence microscopy. Images represent maximum-intensity projections of z stacks (9 planes, 0.3-μm steps).

(C) Percentage of cells with foci was determined in cells treated as in (A) (n > 100). Values represent the mean + SEM of three independent experiments.

(D) Active, GTP-bound Rho1 levels are restored during recovery at 25°C. Cells were heat shocked at 37°C for 1 h or 42°C for 15 min and incubated at 25°C in the presence of CHX for 2 h. Levels of Rho1.C17R-GFP loaded with GTP in whole-cell extracts were assayed by pull-down using recombinant GST-RBD (Rho binding domain) beads. Rho1.C17R-GFP protein was detected in the elution samples (pull-down) and whole-cell extracts (inputs) after immunoblotting with an antibody against GFP. Staining with Ponceau shows levels of recombinant GST-RBD.

Scale bar, 5 μm.

Mayor, is also a thermo-sensitive reporter (Khosrow-Khavar et al., 2012). We cloned *GUK1-9-GFP* under the control of a constitutive promoter and integrated it at the *leu1-32* locus of fission yeast. As shown in Figure 6A, both reporters display dual cytosolic and nuclear localization at 25°C and form foci upon heat shock imposition. Coalescence of these new reporters into PACs relies, totally or partially, on Mas5 and Hsp104, respectively (Figure 6B). Addition of CHX (but not PUR) totally (37°C) or partially (42°C) blocks PAC formation of both Ura4.L261P-GFP and Guk1-9-GFP (Figure S6A).

Second, to monitor whether other endogenous proteins, prone to misfolding, could assemble into these aggregate-like centers upon heat shock in fission yeast, we monitored the localization of the small chaperone Hsp16 in wild-type cells, without co-expression of Rho1.C17R-GFP. As shown in Figure 6C, Hsp16-GFP displays cytosolic/nuclear localization at 25°C and forms 2–3 foci in the cytosol (not in the nucleus) 60 min after shifting cells to 37°C. At 42°C, Hsp16 foci formation occurs immediately, with numerous PACs that are maintained until 60 min. Hsp16-GFP coalescence into PACs is also abolished in the presence of CHX (Figure 6D) or in the absence of Mas5 (Figure 6E). All these findings are recapitulated using Hsp104-GFP as an alternative chaperone labeling PACs (Figures S6B–S6D). This suggests that endogenous fission yeast proteins assemble into PACs upon heat shock in a translation- and Mas5-dependent manner, which are decorated with Hsp16 and other chaperones, as described above for the thermo-sensitive reporters.

Finally, we have carried out proteomic studies to identify the thermo-unstable proteome fraction in fission yeast. We have performed biochemical separation of pellet fractions by centrifugation of whole-cell extracts from wild-type cultures grown at different temperatures, and performed untagged liquid chromatography coupled to tandem MS (LC-MS/MS) of biological triplicates (Figure 7A). We isolated 1,032, 1,135, and 1,228 proteins in the insoluble fractions of extracts from cells grown at 30°C, 37°C, or 42°C, respectively (Figure 7B). A total of 751 proteins were common to the 3 conditions, of which 50 displayed more than a 2-fold change in both heat-stressed samples compared to 30°C; we consider these proteins as part of the thermo-unstable proteome and are shown with green dots in the volcano plots in Figure 7C. To these proteins, we added 160 that were only present in the pellet fractions of extracts from cells grown at 37°C and 42°C but not at 30°C (Figure 7B); we have assigned maximum fold changes to these proteins (indicated with asterisks in the right corners of Figure 7C). Therefore, we conclude that the *S. pombe* thermo-unstable proteome, composed of endogenous proteins enriched in the insoluble fractions of 37°C and 42°C, contains around 210 proteins; among them, we have identified several chaperones (magenta dots in Figure 7C). These proteins were mainly present in the cytosol and nucleus and were distributed into different Gene Ontology categories, with response to stress, amino acid metabolism, and protein catabolic process being highly represented (Figures S7A–S7C). We chose one of them, Hrb1 (labeled with a magenta dot in Figure 7C), as a proof-of-concept: endogenously tagged Hrb1-GFP displays a cytosolic/nuclear distribution at 25°C, and it forms PACs at both 37°C and 42°C only in the absence of CHX, and in a Mas5-dependent manner (Figures 7D and S7D).

In conclusion, PAC formation is also observed in wild-type cells, as demonstrated with the Hsp16-GFP chimera and with the identification of the fraction of thermally sensitive fission yeast proteins. We propose that, in all cases, PAC assembly prevents the UPS-mediated degradation of the reversibly misfolded proteins so that they can be re-solubilized and facilitate growth resumption (Figure 7E).

DISCUSSION

When proteostasis is challenged by heat shock, signaling cascades induce changes that traditionally have been linked to the refolding (through chaperones) and/or degradation (through UPS or autophagy) of the misfolded proteins. Here, we have demonstrated that cytosolic aggregation-prone protein reporters form PACs upon mild (non-toxic) and severe temperature up-shifts as a first line of action of the PQC. This observation could be a specific feature of expressing temperature-sensitive mutant proteins, such as Rho1.C17R-GFP, Ura4.L261P-GFP, or Guk1-9-GFP, so that these specific mutations could destabilize protein structure and render proteins at the boundary of solubility and, therefore, be highly prone to heat-dependent misfolding and aggregation. However, chaperones Hsp16 and Hsp104 follow the same profile and kinetics of foci formation even in wild-type cells, indicating that a fraction of the proteome, including misfolding-prone polypeptides, follows the same chaperone-mediated PAC assembly to avoid degradation by the UPS and to facilitate growth resumption during stress recovery. We have identified this thermo-sensitive fraction by LC-MS/MS, and around 4% of the fission yeast proteome turns into an insoluble fraction during heat shock.

PAC assembly is probably specific for cytosolic clients. Our three reporters were selected by their cytosolic distribution, although they also display nuclear localization. Tethering the temperature-sensitive Rho1 reporter to the membrane abolishes PAC assembly, probably by avoiding cross-interaction (and mutual PAC seeding) with other misfolded GFP-Rho1.C17R molecules. PAC assembly seems to start at the cytosol: the 2–4 foci formed at 37°C never seem to be localized in the nucleus (Figures 1C and 1F). At 42°C, PAC assembly is faster than at 37°C, and there is a higher number of foci. With the exception of Mas5, most chaperones seem to be dispensable for PAC formation at 42°C, and at this temperature CHX addition does not fully block aggregate formation, suggesting that the more dramatic exposure of hydrophobic patches in aggregation-prone proteins that occurs at 42°C may be sufficient to induce their self-aggregation (Figure 7E). At this higher temperature, foci formation occurs both at the cytosol and the nucleus (see inside panels of Figure S6B). We are currently investigating whether these 42°C-dependent foci of Hsp104 and aggregated proteins are located at the nucleolus (Tani et al., 1996), at the nucleoplasma, or in a different location. Even though they differ in their origin, the fate of 37°C and 42°C PACs is common: refolding during stress recovery in an Hsp104-dependent manner (Figure 5). Reversible aggregation of specific proteins, such as Cdc19, may represent a strategy to allow metabolic re-programming during environmental changes, including growth at 42°C (Prouteau and Loewith, 2018; Saad et al., 2017); we propose that formation of

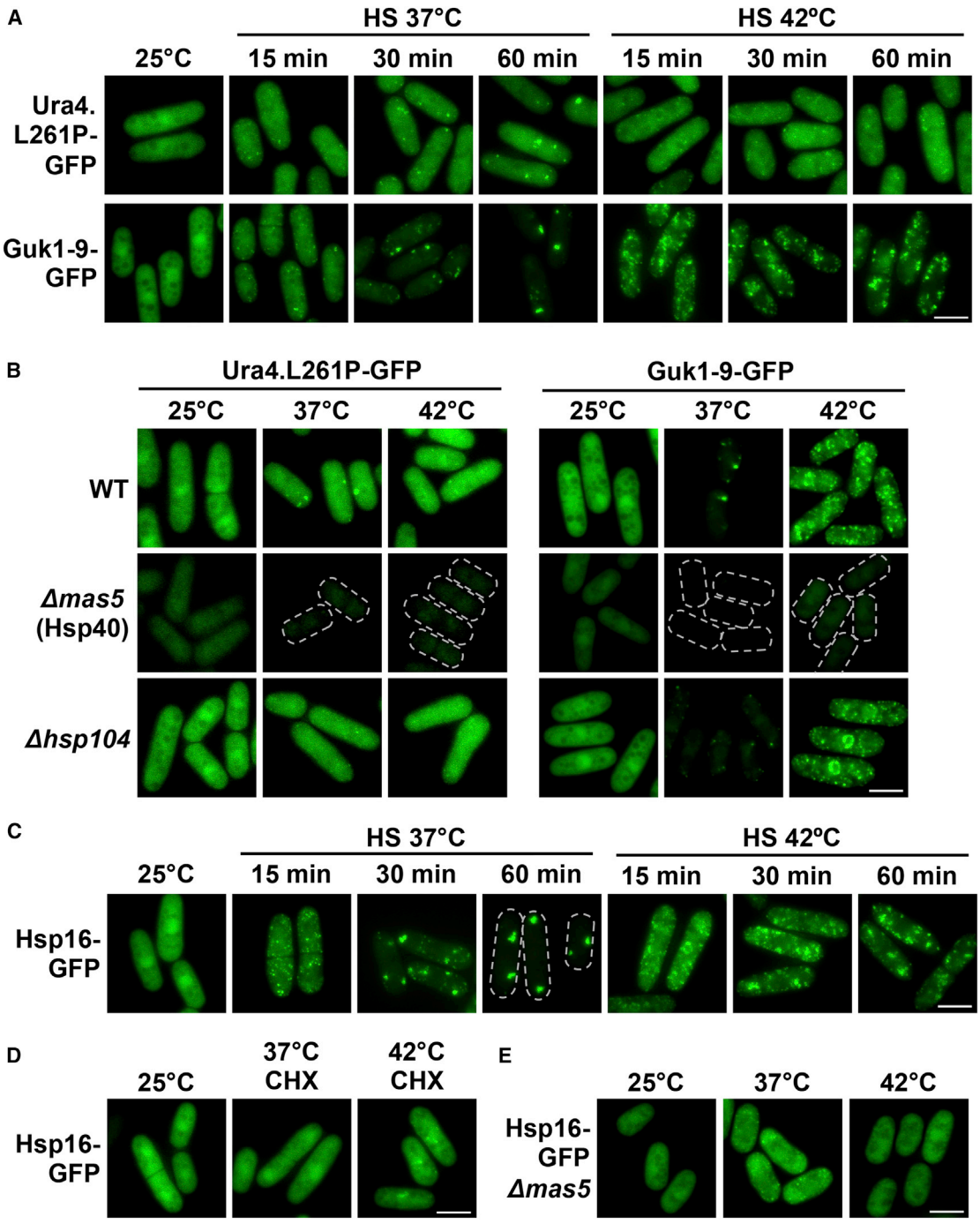

Figure 6. Other Temperature-Sensitive Reporters and Endogenous Proteins Assemble into PACs upon Heat Shock in a Mas5-Dependent Manner

(A) Mild and severe heat stress triggers the formation of PACs containing Ura.L261P and Guk1 mutants. Maximum-intensity projections of z stacks (6 planes, 0.4-μm steps) are shown.

(B) Mas5 chaperone is essential for PAC assembly during heat shock. WT, *Δmas5*, and *Δhsp104* strains expressing Ura4.L261P-GFP or Guk1-9-GFP were incubated at 37°C for 1 h or 42°C for 15 min.

(C) Hsp16 labels PACs carrying endogenous thermo-sensitive proteins. Cells expressing Hsp16-GFP were analyzed by fluorescence microscopy upon heat shock. Images represent maximum-intensity projections of z stacks (6 planes, 0.4-μm steps).

(D and E) CHX and lack of Mas5 abolish the formation of Hsp16-positive PACs. WT (D) or *Δmas5* (E) cells expressing Hsp16-GFP were heat shocked at 37°C for 1 h or 42°C for 15 min. Where indicated, CHX was added to inhibit translation.

Dashed lines indicate the borders of yeast cells. Scale bar, 5 μm. See also Figure S6.

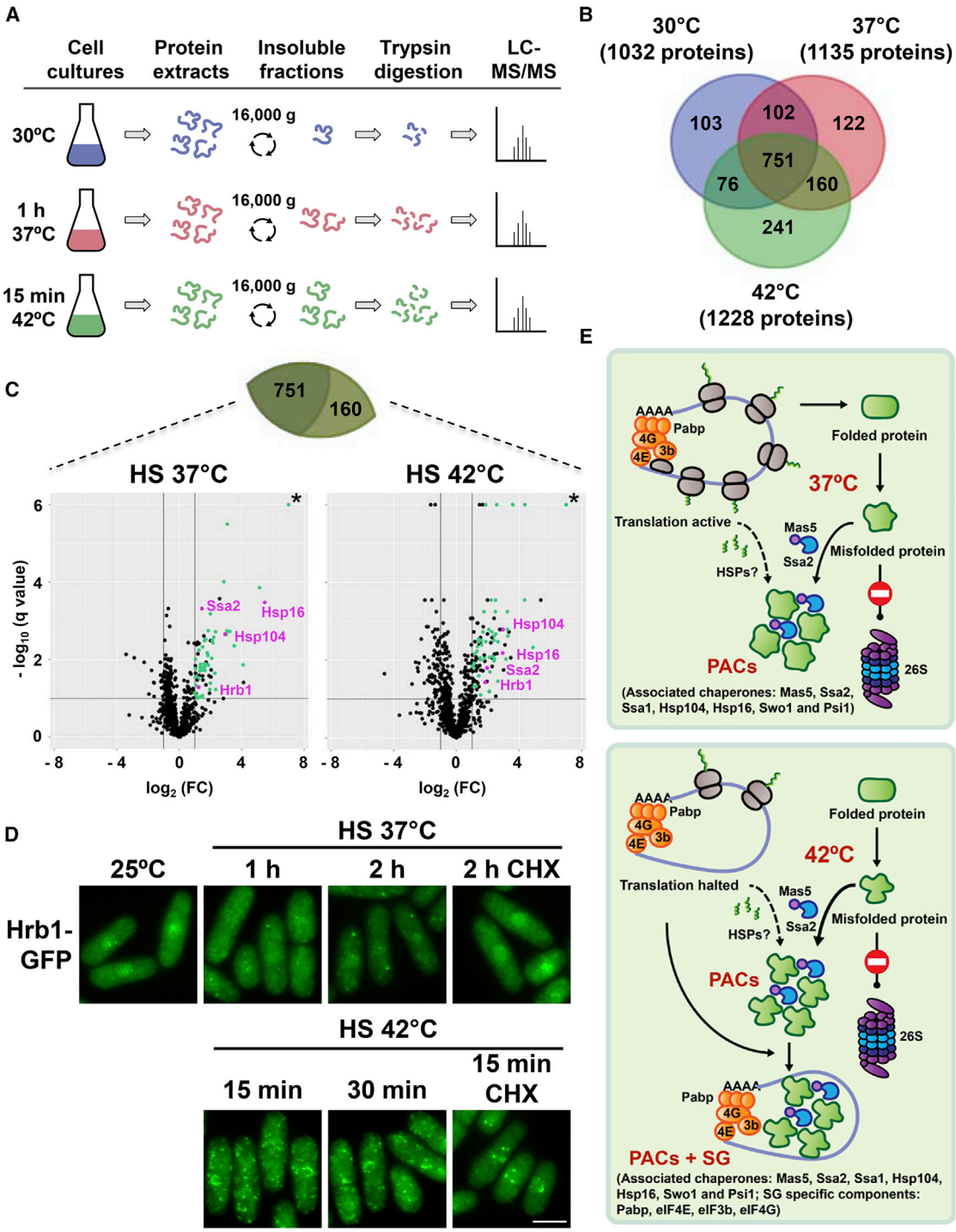

Figure 7. Identification of the Thermo-Unstable Proteome of Fission Yeast by MS

(A) Experimental design to identify insoluble proteins by MS. Protein extracts from cell cultures treated as indicated were centrifuged to isolate insoluble fractions. Proteins enriched in these fractions were subjected to trypsin digestion and identified by label-free LC-MS/MS.

(B) Venn diagram of the overlap between insoluble proteins identified at each growth condition. In total, 751 + 160 proteins were identified in the insoluble fractions of both 37°C and 42°C heat-shocked cells.

(C) Log_2 fold changes (FCs) in protein abundance after heat stress at 37°C or 42°C in comparison with growth at 30°C. Volcano plots include 751 + 160 insoluble proteins at 37°C and 42°C. A total of 50 proteins with statistically significant changes for both treatments ($log_2FC \geq 1$, q value ≤ 0.1) are labeled in green. The 160

(legend continued on next page)

severe heat-shock-dependent PACs may contribute to the deposition, among other thermo-sensitive proteins, of these metabolic enzymes.

Is PAC assembly at specific cellular sites a chaperone-mediated process? We propose that it is. This seems to be the role of the Hsp40 Mas5, probably combined with Ssa2. During nucleation of aggregates, Mas5 would sequester clients, in reparable stages of unfolding, probably preserving a native-like central structure; insertion of Mas5 moieties between the misfolded substrates would keep them apart, preventing an irreversible aggregation state (Figure 7E). A role similar to this one has been proposed at extreme temperatures for the budding yeast chaperone Hsp42, with an N-terminal prion-like domain holding the chaperone's aggregase activity (Mogk and Bukau, 2017; Specht et al., 2011). Once stress conditions would permit, disaggregases, such as Hsp104, would facilitate aggregate dissolution and protein refolding. Another important observation about *Δmas5* cells is that the concentration of temperature-sensitive proteins, such as that of our three reporters, is significantly lower than in wild-type cells even at a permissive temperature (Figures 2 and 6B). We propose that Mas5 is one of the PQC components recognizing hydrophobic patches and actively maintaining the native structure of aggregation-prone proteins during physiological conditions, so that in its absence these proteins would be degraded. During heat shock, the folding activity of Mas5 may be overcome, either through ATP depletion or by the enhanced number of unfolded clients; the promiscuous interaction of Mas5 with partially unfolded proteins would then generate aggregate-like structures, the PACs, to prevent their massive degradation and/or irreversible unfolding.

During the course of our study, we studied the effect of new protein synthesis on PAC assembly. Newly translated proteins, which are being synthesized at polysomes, are more prone to aggregation than terminated proteins, and the former may serve as seeds to cytosolic clients that are more resilient to misfold. As shown in Figure 4, addition of CHX fully blocks PAC formation at 37°C (and only partially at 42°C), whereas PUR has no negative effect on PAC assembly. CHX inhibits translation by blocking the peptidyl transferase activity of the 60S ribosome subunit and, therefore, halts the elongation process and probably "freezes" all the translation components together, including mRNAs covered with ribosomes, non-full-length polypeptides, translation initiation factors, and ribosomal PQC components. On the contrary, PUR causes premature termination of translation, therefore releasing free to the cytosol all those translation elements. Which of these components arising from the translation machinery (e.g., defective protein products and HSPs acting at *de novo* synthesis level) are required to initiate PAC seeding is still to be determined (Figure 7E). So far, we know that a lack of the ribosomal Hsp70 Sks2 or the RAC components Ssz1 or Zuo1 have a small but significant defect in PAC assembly at 37°C. It is not surprising that components of another ribosomal PQC complex, the NAC, are not required for the assembly of cytosolic misfolded proteins into PACs (Figure S2A). At least in budding yeast, the highly conserved NAC dimer has been cross-linked to very short nascent chains and to the signal-recognition particle (SRP) complex, which drives translated mRNAs to the endoplasmic reticulum surface (del Alamo et al., 2011).

We have demonstrated here that a secondary fate of cytosolic misfolded substrates is degradation by the UPS. We have also noticed that upon heat shock, approximately two-thirds of the total Rho1.C17R-GFP forms PACs, whereas one-third is degraded by the proteasome, as demonstrated using the proteasome inhibitor BZ (Figure 4G). We propose, based on our thermo-sensitive reporter, that upon heat shock a fraction of the pool of the misfolded protein is sent to degradation and non-irreversibly misfolded molecules are sent to PACs for future refolding (Figure 7E). We have identified San1 as the E3 ubiquitin ligase labeling some, but not all, cytosolic/nuclear misfolded substrates for degradation, and we are currently working to identify other E3 ligases and UPS components involved in this process.

We have shown here that PAC formation is a heat shock adaptation response in fission yeast. In *S. cerevisiae,* the fate of heat-shock-dependent aggregation centers (JUNQs and IPODs) had been proposed to be degradation (Escusa-Toret et al., 2013; Kaganovich et al., 2008), although this model has been challenged by other reports (Miller et al., 2015; Wallace et al., 2015). Our work in fission yeast is in good agreement with the later: protein sequestration into PACs is a general strategy to protect them from degradation. Importantly, we demonstrate that PACs protect the thermo-sensitive proteome even when viability has not been challenged, whereas in budding yeast the formation of foci refractory to degradation seems to require harsher conditions (i.e., addition of proteasomal inhibitors or use of extreme temperatures). Our current view is that the heat-shock-challenged PQC system in fission yeast tries to ensure a healthy and stable proteome by refolding, degrading, or sequestering misfolded proteins into PACs, which can be later on disaggregated and may promote re-adaptation.

STAR★METHODS

Detailed methods are provided in the online version of this paper and include the following:

- KEY RESOURCES TABLE
- LEAD CONTACT AND MATERIALS AVAILABILITY
- EXPERIMENTAL MODEL AND SUBJECT DETAILS
- METHOD DETAILS
  - Yeast strains, plasmids and molecular biology
  - Drug treatments
  - Growth curves
  - Spots assay

proteins only found in the insoluble fractions of both 37°C and 42°C extracts are indicated as a single dot and an asterisk in the right corner of both panels. Chaperones and RNA-binding protein Hrb1 are shown as magenta dots.

(D) The Hrb1 protein is present at PACs. Distribution of Hrb1-GFP was monitored by fluorescence microscopy upon heat shock at 37°C and 42°C for the indicated time points. CHX treatment abolishes the formation of Hrb1-positive aggregates during heat stress.

(E) Model depicting the formation of PACs during the cell response to heat stress. See Discussion for details.

Scale bar, 5 μm. See also Figure S7.

SUPPLEMENTAL INFORMATION

Supplemental Information can be found online at https://doi.org/10.1016/j.celrep.2020.01.077.

ACKNOWLEDGMENTS

We thank Snezhana Oliferenko, Iva Tolic, Thibault Mayor, John Davey, Graham Ladds, Shao-Win Wang, and Ken Sawin for providing strains and plasmids. We also thank Shao-Win Wang for advice on the detection of SGs, Guadalupe Espadas from CRG/UPF Proteomic Unit for performing the MS experiments, and David Castillo for support in statistical analysis. This work is supported by the Ministerio de Ciencia, Innovación y Universidades, PLAN E, and FEDER (Spain) (PGC2018-093920-B-I00 to E.H. and BFU2016-75116-P to M.C.). The Oxidative Stress and Cell Cycle group is also supported by Generalitat de Catalunya (Spain) (2017-SGR-539) and by Unidad de Excelencia María de Maeztu from MINECO (Spain) (MDM-2014-0370). M.C. is funded by the Ramon y Cajal program (MINECO-RYC2013-12858). E.H. is a recipient of an ICREA Academia Award (Generalitat de Catalunya, Spain).

AUTHOR CONTRIBUTIONS

M.C., S.B., and L.M. performed most experiments. M.C., S.B., L.M., M.V., P.P., J.A., and E.H. analyzed the data. E.H. wrote the manuscript.

DECLARATION OF INTERESTS

The authors declare no competing interests.

Received: June 19, 2019
Revised: October 18, 2019
Accepted: January 22, 2020
Published: February 18, 2020

REFERENCES

Alfa, C., Fantes, P., Hyams, J., McLeod, M., and Warbrick, E. (1993). Experiments with Fission Yeast: A Laboratory Course Manual (Cold Spring Harbor Laboratory).

Amm, I., Sommer, T., and Wolf, D.H. (2014). Protein quality control and elimination of protein waste: the role of the ubiquitin-proteasome system. Biochim. Biophys. Acta *1843*, 182–196.

Arellano, M., Coll, P.M., Yang, W., Duran, A., Tamanoi, F., and Perez, P. (1998). Characterization of the geranylgeranyl transferase type I from Schizosaccharomyces pombe. Mol. Microbiol. *29*, 1357–1367.

Bähler, J., Wu, J.Q., Longtine, M.S., Shah, N.G., McKenzie, A., 3rd, Steever, A.B., Wach, A., Philippsen, P., and Pringle, J.R. (1998). Heterologous modules for efficient and versatile PCR-based gene targeting in *Schizosaccharomyces pombe*. Yeast *14*, 943–951.

Balchin, D., Hayer-Hartl, M., and Hartl, F.U. (2016). *In vivo* aspects of protein folding and quality control. Science *353*, aac4354.

Beer, L.A., Liu, P., Ky, B., Barnhart, K.T., and Speicher, D.W. (2017). Efficient Quantitative Comparisons of Plasma Proteomes Using Label-Free Analysis with MaxQuant. Methods Mol. Biol. *1619*, 339–352.

Benson, F.E., Stasiak, A., and West, S.C. (1994). Purification and characterization of the human Rad51 protein, an analogue of *E. coli* RecA. EMBO J. *13*, 5764–5771.

Bounedjah, O., Desforges, B., Wu, T.D., Pioche-Durieu, C., Marco, S., Hamon, L., Curmi, P.A., Guerquin-Kern, J.L., Piétrement, O., and Pastré, D. (2014). Free mRNA in excess upon polysome dissociation is a scaffold for protein multimerization to form stress granules. Nucleic Acids Res. *42*, 8678–8691.

Cherkasov, V., Hofmann, S., Druffel-Augustin, S., Mogk, A., Tyedmers, J., Stoecklin, G., and Bukau, B. (2013). Coordination of translational control and protein homeostasis during severe heat stress. Curr. Biol. *23*, 2452–2462.

Coelho, M., Lade, S.J., Alberti, S., Gross, T., and Tolić, I.M. (2014). Fusion of protein aggregates facilitates asymmetric damage segregation. PLoS Biol. *12*, e1001886.

Coll, P.M., Trillo, Y., Ametzazurra, A., and Perez, P. (2003). Gef1p, a new guanine nucleotide exchange factor for Cdc42p, regulates polarity in *Schizosaccharomyces pombe*. Mol. Biol. Cell *14*, 313–323.

Davis, K., Pateman, C., and Davey, J. (1999). Gene disruption in *Schizosaccharomyces pombe* using a temperature-sensitive Ura4p. Yeast *15*, 1231–1236.

del Alamo, M., Hogan, D.J., Pechmann, S., Albanese, V., Brown, P.O., and Frydman, J. (2011). Defining the specificity of cotranslationally acting chaperones by systematic analysis of mRNAs associated with ribosome-nascent chain complexes. PLoS Biol. *9*, e1001100.

Dikic, I. (2017). Proteasomal and Autophagic Degradation Systems. Annu. Rev. Biochem. *86*, 193–224.

Erjavec, N., Larsson, L., Grantham, J., and Nyström, T. (2007). Accelerated aging and failure to segregate damaged proteins in Sir2 mutants can be suppressed by overproducing the protein aggregation-remodeling factor Hsp104p. Genes Dev. *21*, 2410–2421.

Escusa-Toret, S., Vonk, W.I.M., and Frydman, J. (2013). Spatial sequestration of misfolded proteins by a dynamic chaperone pathway enhances cellular fitness during stress. Nat. Cell Biol. *15*, 1231–1243.

Fernández-Vázquez, J., Vargas-Pérez, I., Sansó, M., Buhne, K., Carmona, M., Paulo, E., Hermand, D., Rodríguez-Gabriel, M., Ayté, J., Leidel, S., and Hidalgo, E. (2013). Modification of tRNA(Lys) UUU by elongator is essential for efficient translation of stress mRNAs. PLoS Genet. *9*, e1003647.

Gloge, F., Becker, A.H., Kramer, G., and Bukau, B. (2014). Co-translational mechanisms of protein maturation. Curr. Opin. Struct. Biol. *24*, 24–33.

Glover, J.R., and Lindquist, S. (1998). Hsp104, Hsp70, and Hsp40: a novel chaperone system that rescues previously aggregated proteins. Cell *94*, 73–82.

Humphrey, T., and Enoch, T. (1998). Sum1, a highly conserved WD-repeat protein, suppresses S-M checkpoint mutants and inhibits the osmotic stress cell cycle response in fission yeast. Genetics *148*, 1731–1742.

Iwaki, T., Giga-Hama, Y., and Takegawa, K. (2006). A survey of all 11 ABC transporters in fission yeast: two novel ABC transporters are required for red pigment accumulation in a *Schizosaccharomyces pombe* adenine biosynthetic mutant. Microbiology *152*, 2309–2321.

Jacobson, T., Navarrete, C., Sharma, S.K., Sideri, T.C., Ibstedt, S., Priya, S., Grant, C.M., Christen, P., Goloubinoff, P., and Tamás, M.J. (2012). Arsenite interferes with protein folding and triggers formation of protein aggregates in yeast. J. Cell Sci. *125*, 5073–5083.

Jara, M., Vivancos, A.P., Calvo, I.A., Moldón, A., Sansó, M., and Hidalgo, E. (2007). The peroxiredoxin Tpx1 is essential as a H2O2 scavenger during aerobic growth in fission yeast. Mol. Biol. Cell *18*, 2288–2295.

Kaganovich, D., Kopito, R., and Frydman, J. (2008). Misfolded proteins partition between two distinct quality control compartments. Nature *454*, 1088–1095.

Kampmeyer, C., Karakostova, A., Schenstrøm, S.M., Abildgaard, A.B., Lauridsen, A.M., Jourdain, I., and Hartmann-Petersen, R. (2017). The exocyst subunit Sec3 is regulated by a protein quality control pathway. J. Biol. Chem. *292*, 15240–15253.

Kedersha, N., Cho, M.R., Li, W., Yacono, P.W., Chen, S., Gilks, N., Golan, D.E., and Anderson, P. (2000). Dynamic shuttling of TIA-1 accompanies the recruitment of mRNA to mammalian stress granules. J. Cell Biol. *151*, 1257–1268.

Khosrow-Khavar, F., Fang, N.N., Ng, A.H., Winget, J.M., Comyn, S.A., and Mayor, T. (2012). The yeast ubr1 ubiquitin ligase participates in a prominent pathway that targets cytosolic thermosensitive mutants for degradation. G3 (Bethesda) *2*, 619–628.

Kim, Y.E., Hipp, M.S., Bracher, A., Hayer-Hartl, M., and Hartl, F.U. (2013). Molecular chaperone functions in protein folding and proteostasis. Annu. Rev. Biochem. *82*, 323–355.

Kleiger, G., and Mayor, T. (2014). Perilous journey: a tour of the ubiquitin-proteasome system. Trends Cell Biol. *24*, 352–359.

Kriegenburg, F., Jakopec, V., Poulsen, E.G., Nielsen, S.V., Roguev, A., Krogan, N., Gordon, C., Fleig, U., and Hartmann-Petersen, R. (2014). A chaperone-assisted degradation pathway targets kinetochore proteins to ensure genome stability. PLoS Genet. *10*, e1004140.

Kroschwald, S., Maharana, S., Mateju, D., Malinovska, L., Nüske, E., Poser, I., Richter, D., and Alberti, S. (2015). Promiscuous interactions and protein disaggregases determine the material state of stress-inducible RNP granules. eLife *4*, e06807.

Leupold, U. (1970). Genetical methods for *Schizosaccharomyces pombe*. In: Methods Cell Physiol.*4* (D.M.Prescott), pp. 169–177.

Mathiassen, S.G., Larsen, I.B., Poulsen, E.G., Madsen, C.T., Papaleo, E., Lindorff-Larsen, K., Kragelund, B.B., Nielsen, M.L., Kriegenburg, F., and Hartmann-Petersen, R. (2015). A Two-step Protein Quality Control Pathway for a Misfolded DJ-1 Variant in Fission Yeast. J. Biol. Chem. *290*, 21141–21153.

Matsuo, Y., Kishimoto, H., Tanae, K., Kitamura, K., Katayama, S., and Kawamukai, M. (2011). Nuclear protein quality is regulated by the ubiquitin-proteasome system through the activity of Ubc4 and San1 in fission yeast. J. Biol. Chem. *286*, 13775–13790.

Miller, S.B., Ho, C.T., Winkler, J., Khokhrina, M., Neuner, A., Mohamed, M.Y., Guilbride, D.L., Richter, K., Lisby, M., Schiebel, E., et al. (2015). Compartment-specific aggregases direct distinct nuclear and cytoplasmic aggregate deposition. EMBO J. *34*, 778–797.

Mogk, A., and Bukau, B. (2017). Role of sHsps in organizing cytosolic protein aggregation and disaggregation. Cell Stress Chaperones *22*, 493–502.

Mogk, A., Kummer, E., and Bukau, B. (2015). Cooperation of Hsp70 and Hsp100 chaperone machines in protein disaggregation. Front. Mol. Biosci. *2*, 22.

Mollet, S., Cougot, N., Wilczynska, A., Dautry, F., Kress, M., Bertrand, E., and Weil, D. (2008). Translationally repressed mRNA transiently cycles through stress granules during stress. Mol. Biol. Cell *19*, 4469–4479.

Nillegoda, N.B., Wentink, A.S., and Bukau, B. (2018). Protein Disaggregation in Multicellular Organisms. Trends Biochem. Sci. *43*, 285–300.

Nilsson, D., and Sunnerhagen, P. (2011). Cellular stress induces cytoplasmic RNA granules in fission yeast. RNA *17*, 120–133.

Park, H.O., and Bi, E. (2007). Central roles of small GTPases in the development of cell polarity in yeast and beyond. Microbiol. Mol. Biol. Rev. *71*, 48–96.

Pechmann, S., Willmund, F., and Frydman, J. (2013). The ribosome as a hub for protein quality control. Mol. Cell *49*, 411–421.

Penney, M., Samejima, I., Wilkinson, C.R., McInerny, C.J., Mathiassen, S.G., Wallace, M., Toda, T., Hartmann-Petersen, R., and Gordon, C. (2012). Fission yeast 26S proteasome mutants are multi-drug resistant due to stabilization of the Pap1 transcription factor. PLoS One *7*, e50796.

Pérez, P., and Cansado, J. (2010). Cell integrity signaling and response to stress in fission yeast. Curr. Protein Pept. Sci. *11*, 680–692.

Perkins, D.N., Pappin, D.J., Creasy, D.M., and Cottrell, J.S. (1999). Probability-based protein identification by searching sequence databases using mass spectrometry data. Electrophoresis *20*, 3551–3567.

Pilla, E., Schneider, K., and Bertolotti, A. (2017). Coping with Protein Quality Control Failure. Annu. Rev. Cell Dev. Biol. *33*, 439–465.

Prouteau, M., and Loewith, R. (2018). Regulation of Cellular Metabolism through Phase Separation of Enzymes. Biomolecules *8*, E160.

Saad, S., Cereghetti, G., Feng, Y., Picotti, P., Peter, M., and Dechant, R. (2017). Reversible protein aggregation is a protective mechanism to ensure cell cycle restart after stress. Nat. Cell Biol. *19*, 1202–1213.

Sánchez-Mir, L., Franco, A., Martín-García, R., Madrid, M., Vicente-Soler, J., Soto, T., Gacto, M., Pérez, P., and Cansado, J. (2014). Rho2 palmitoylation is required for plasma membrane localization and proper signaling to the fission yeast cell integrity mitogen- activated protein kinase pathway. Mol. Cell. Biol. *34*, 2745–2759.

Satoh, R., Tanaka, A., Kita, A., Morita, T., Matsumura, Y., Umeda, N., Takada, M., Hayashi, S., Tani, T., Shinmyozu, K., and Sugiura, R. (2012). Role of the RNA-binding protein Nrd1 in stress granule formation and its implication in the stress response in fission yeast. PLoS One *7*, e29683.

Schindelin, J., Arganda-Carreras, I., Frise, E., Kaynig, V., Longair, M., Pietzsch, T., Preibisch, S., Rueden, C., Saalfeld, S., Schmid, B., et al. (2012). Fiji: an open-source platform for biological-image analysis. Nat. Methods *9*, 676–682.

Shannon, P., Markiel, A., Ozier, O., Baliga, N.S., Wang, J.T., Ramage, D., Amin, N., Schwikowski, B., and Ideker, T. (2003). Cytoscape: a software environment for integrated models of biomolecular interaction networks. Genome Res. *13*, 2498–2504.

Snaith, H.A., Samejima, I., and Sawin, K.E. (2005). Multistep and multimode cortical anchoring of tea1p at cell tips in fission yeast. EMBO J. *24*, 3690–3699.

Sontag, E.M., Samant, R.S., and Frydman, J. (2017). Mechanisms and Functions of Spatial Protein Quality Control. Annu. Rev. Biochem. *86*, 97–122.

Specht, S., Miller, S.B., Mogk, A., and Bukau, B. (2011). Hsp42 is required for sequestration of protein aggregates into deposition sites in Saccharomyces cerevisiae. J. Cell Biol. *195*, 617–629.

Takeda, K., and Yanagida, M. (2005). Regulation of nuclear proteasome by Rhp6/Ubc2 through ubiquitination and destruction of the sensor and anchor Cut8. Cell *122*, 393–405.

Tani, T., Derby, R.J., Hiraoka, Y., and Spector, D.L. (1996). Nucleolar accumulation of poly (A)+ RNA in heat-shocked yeast cells: implication of nucleolar involvement in mRNA transport. Mol. Biol. Cell *7*, 173–192.

Viana, R.A., Pinar, M., Soto, T., Coll, P.M., Cansado, J., and Pérez, P. (2013). Negative functional interaction between cell integrity MAPK pathway and Rho1 GTPase in fission yeast. Genetics *195*, 421–432.

Vivancos, A.P., Castillo, E.A., Biteau, B., Nicot, C., Ayté, J., Toledano, M.B., and Hidalgo, E. (2005). A cysteine-sulfinic acid in peroxiredoxin regulates H2O2-sensing by the antioxidant Pap1 pathway. Proc. Natl. Acad. Sci. USA *102*, 8875–8880.

Vizcaíno, J.A., Csordas, A., del-Toro, N., Dianes, J.A., Griss, J., Lavidas, I., Mayer, G., Perez-Riverol, Y., Reisinger, F., Ternent, T., et al. (2016). 2016 update of the PRIDE database and its related tools. Nucleic Acids Res. *44*, D447–D456.

Vjestica, A., Zhang, D., Liu, J., and Oliferenko, S. (2013). Hsp70-Hsp40 chaperone complex functions in controlling polarized growth by repressing Hsf1-driven heat stress-associated transcription. PLoS Genet. *9*, e1003886.

Wallace, E.W., Kear-Scott, J.L., Pilipenko, E.V., Schwartz, M.H., Laskowski, P.R., Rojek, A.E., Katanski, C.D., Riback, J.A., Dion, M.F., Franks, A.M., et al. (2015). Reversible, Specific, Active Aggregates of Endogenous Proteins Assemble upon Heat Stress. Cell *162*, 1286–1298.

Wang, C.Y., Wen, W.L., Nilsson, D., Sunnerhagen, P., Chang, T.H., and Wang, S.W. (2012). Analysis of stress granule assembly in *Schizosaccharomyces pombe*. RNA *18*, 694–703.

Wen, W.L., Stevenson, A.L., Wang, C.Y., Chen, H.J., Kearsey, S.E., Norbury, C.J., Watt, S., Bähler, J., and Wang, S.W. (2010). Vgl1, a multi-KH domain protein, is a novel component of the fission yeast stress granules required for cell survival under thermal stress. Nucleic Acids Res. *38*, 6555–6566.

Zhou, C., Slaughter, B.D., Unruh, J.R., Guo, F., Yu, Z., Mickey, K., Narkar, A., Ross, R.T., McClain, M., and Li, R. (2014). Organelle-based aggregation and retention of damaged proteins in asymmetrically dividing cells. Cell *159*, 530–542.

STAR★METHODS

KEY RESOURCES TABLE

REAGENT or RESOURCE	SOURCE	IDENTIFIER
Antibodies		
Rabbit polyclonal anti-Sty1	Jara et al., 2007	N/A
Mouse monoclonal anti-GFP	Takara	Cat# 632381; RIDD: AB_2313808
Bacterial and Virus Strains		
E.coli FB810	Benson et al., 1994	N/A
Chemicals, Peptides, and Recombinant Proteins		
Cycloheximide	Sigma-Aldrich	Cat# C7698
Bortezomid	LC Laboratories	Cat# B-1408
Anisomycin	Sigma-Aldrich	Cat# A9789
Puromycin	Sigma-Aldrich	Cat# P8833
GST-C21RBD	Coll et al., 2003	N/A
Deposited Data		
MS data	This paper	PRIDE database: PXD014400
Images	This paper; Mendeley Data	https://doi.org/10.17632/fxxynrt6hj.1
Experimental Models: Organisms/Strains		
S.pombe background strain 972	Leupold, 1970	N/A
S.pombe background strain HM123	Lab stock	N/A
Other strains see Table S1		
Recombinant DNA		
Plasmid *sty1-Rho1-GFP*	This paper	N/A
Plasmid *sty1-Rho1.C17R-GFP*	This paper	N/A
Plasmid *sty1-Rho1.C17R-mCherry*	This paper	N/A
Plasmid *sty1-GFP-Rho1*	This paper	N/A
Plasmid *sty1-GFP-Rho1.C17R*	This paper	N/A
Plasmid *sty1-GFP-C17R.C199S*	This paper	N/A
Plasmid *sty1-Guk1-9-GFP*	This paper	N/A
Plasmid *sty1-GFP-Psi1*	This paper	N/A
Plasmid pGEX-C21RBD	Coll et al., 2003	N/A
Software and Algorithms		
Fiji/ImageJ	Schindelin et al., 2012	https://fiji.sc/
Cytoscape	Shannon et al., 2003	https://cytoscape.org
Venn Plotter	VIB / UGent Bioinformatics & Evolutionary Genomics	http://bioinformatics.psb.ugent.be/webtools/Venn/
Image Studio Lite	Li-Cor Biosciences	https://www.licor.com/bio/image-studio-lite/

LEAD CONTACT AND MATERIALS AVAILABILITY

Further information and requests for resources and reagents should be directed to and will be fulfilled by the Lead Contact, Elena Hidalgo (elena.hidalgo@upf.edu). This study did not generate new unique reagents.

EXPERIMENTAL MODEL AND SUBJECT DETAILS

Wild-type and Δ*sty1* fission yeast strains were grown in rich medium (YE5S) at 30°C as described previously (Alfa et al., 1993). Yeast cells expressing temperature-sensitive mutants were grown in minimal medium (MM) at 25°C before incubation at restrictive temperatures 37°C, 42°C or 46°C. The genotypes of strains used in this study are shown in Table S1.

METHOD DETAILS

Yeast strains, plasmids and molecular biology

The construction of most deletion and tagging of genes was done using homologous recombination with PCR fragments, using as templates pFA6a plasmid derivatives (Bähler et al., 1998). Regarding the construction of tagged Hsp104, only some fusion proteins remained functional, as shown by measuring cell survival on solid plates upon heat shock imposition (Figure S1D); most Hsp104-tagged strains were constructed as described above with the exception of Hsp104-GFP, derived from a strain provided by Dr. Oliferenko (Vjestica et al., 2013), and Hsp104-GFP* provided by Dr. Tolic (Coelho et al., 2014); this last chimera was not fully functional (Figure S1D). To obtain the strain expressing Ura4.L261P, a PCR fragment was amplified from genomic DNA with a primer containing the point mutation. Plasmids containing N-terminally GFP-tagged Rho1 and Rho1.C17R under the control of the constitutive *sty1* promoter (Fernández-Vázquez et al., 2013) were generated from pJK148-Rho1 and Rho1-596 plasmids (Viana et al., 2013). Plasmids containing C-terminally GFP-tagged Rho1 and Rho1.C17R under the control of the constitutive *sty1* promoter were derived from plasmid pREP41-Hmt1-GFP (provided by Kaoru Takegawa, Kyushu University, Japan) (Iwaki et al., 2006). Plasmid with C-terminal mCherry was obtained by replacement of GFP by mCherry sequence amplified from pFA6a-mCherry plasmid (provided by Ken Sawin, University of Edinburgh, UK) (Snaith et al., 2005). Guk1-9 sequence was amplified from genomic DNA of YTM742 strain (provided by Thibault Mayor, University of British Columbia, Canada) (Khosrow-Khavar et al., 2012) and cloned into a plasmid containing *sty1* promoter and C-terminal GFP. Plasmid pGEX-RBD (Rho binding domain) was used to express in *E. coli* GST fused to Rho binding domain from Rhotekin protein (Coll et al., 2003).

Drug treatments

Cells were incubated with 0.1 mg/ml cycloheximide (Sigma-Aldrich), 0.1 mM bortezomib (LC Labs), 0.2 mg/ml anisomycin (Sigma-Aldrich), or 1 mM puromycin (Sigma-Aldrich).

Growth curves

Cells were grown in YE5S in flasks at different temperatures (30°C, 37°C or 42°C) from an initial OD_{600} of 0.3 during 24 h. To monitor cell growth, optical density was measured every 1-2 h using an Ultraspec 2100 pro spectrophotometer (Amersham Biosciences). One experiment of three replicates is shown.

Spots assay

Cells were grown in YE5S to logarithmic phase (OD_{600} 0.5), concentrated to OD_{600} 2.5, and 1/10 serial dilutions spotted onto plates of rich media. Plates were imaged after three days of growth at 30°C, 37°C or 42°C. Alternatively, liquid cultures were incubated at 30°C, 37°C or 42°C for 6 h before spotting in rich media plates and growth at 30°C.

Microscopy

Cells were grown to logarithmic phase in MM, harvested by centrifugation, and visualized at room temperature. Images were acquired using a Nikon Eclipse 90i microscope equipped with differential interference contrast optics, a PLAN APO VC 100x 1.4 oil immersion objective, an ORCA-II-ERG camera (Hamamatsu), excitation and emission filters GFP-4050B and mCherry-C (Semrock) and image acquisition software Metamorph 7.8.13 (Gataca Systems). Processing of all images was performed using Fiji (ImageJ, National Institutes of Health) (Schindelin et al., 2012). When indicated, to cover a larger volume of the cell, z stacks of 6-9 images with 0.3-0.4 μm spacing were acquired and represented in single images as maximum-intensity projections.

For foci quantification, puncta were identified in 8-bit images using Find Maxima tool of Fiji with a noise tolerance of 15.

Protein solubility assay

Cells from 20 mL culture (OD_{600} 0.5) grown in MM were harvested by centrifugation and resuspended in 250 μl lysis buffer A [20 mM HEPES-KOH pH 7.5, 0.5% NP-40, 200 mM NaCl, 1 mM EDTA, protease inhibitor cocktail, 1 mM PMSF and aprotinin (0.03-0.07 TIU)]. After addition of glass beads, cells were lysed using Vortex Genie 2 (Scientific Industries). Lysates were centrifuged at 2,000 *g* for 5 min at 4°C, and the resulting supernatant (Total, T) was then centrifuged at 16,000 *g* for 10 min to obtain pellet (P) and supernatant (S) fractions. Supernatants and pellets in SDS sample buffer were boiled for 5 min at 95°C, loaded onto 10% SDS-polyacrylamide gel electrophoresis (SDS-PAGE) gels, and subjected to immunoblot analysis.

TCA extracts and immunoblot analysis

Modified trichloroacetic acid (TCA) extracts were prepared as previously described (Vivancos et al., 2005). Samples were separated by SDS-PAGE and detected by immunoblotting with monoclonal anti-GFP (Takara). Anti-Sty1 polyclonal antibody (Jara et al., 2007) was used as loading control.

Purification of recombinant GST-Rho binding domain

GST fused to RBD (Rho binding domain of human Rhotekin protein) (Coll et al., 2003) was expressed in the *E. coli* strain FB810 (Benson et al., 1994) upon addition of 0.5 mM isopropyl 1-thio-β-d-galactopyranoside. 500 mL cultures were grown at 30°C for 4 h, cells

were harvested and sonicated in cold PBS containing 0.4 mg/ml lysozyme, 1 mM PMSF and protease inhibitor cocktail. Lysates were incubated with 400 μl of glutathione agarose beads (Agarose Bead Technologies) for 2 h at 4°C and beads were washed three times with PBS and twice with lysis buffer B (50 mM Tris-HCl pH 7.6, 20 mM NaCl, 0.5% NP-40, 10% glycerol, 2 mM $MgCl_2$, 0.1 mM DTT, protease inhibitor cocktail and 1 mM PMSF), and were finally resuspended in 400 μl of lysis buffer B.

Pull-down assay to measure Rho1-GTP levels

Cells from 50 mL culture (OD_{600} 0.5-0.8) grown in MM were harvested by centrifugation and cell pellets resuspended in 250 μl of lysis buffer B. After addition of glass beads, cells were lysed using a Precellys cell disrupter (Bertin Technologies). The lysate was centrifuged at 2,300 *g* for 10 min and the supernatant (1.7 mg of protein) was incubated with 30 μl of GST-RBD beads for 2 h at 4°C. Beads were isolated by centrifugation at 100 *g* for 1 min at 4°C and washed with lysis buffer B four times. Bound proteins were eluted with SDS sample buffer, boiled for 5 min at 95°C, loaded onto SDS-PAGE gels, and subjected to immunoblot analysis.

Sample preparation for MS experiments

Biological triplicates of pellet fractions from 200 mL cultures (OD_{600} 0.5) grown in MM at 30°C, 37°C or 42°C were obtained as described above (see Protein solubility assay), with the only modification of using a Precellys cell disrupter (Bertin Technologies) to lyse the cell suspensions. After washing twice the pellet fractions with lysis buffer A, 10 μg of each pellet fraction were reduced with dithiothreitol (100 mM, 37°C, 60 min) and alkylated in the dark with iodoacetamide (5 μmol, 25°C, 20 min). The resulting protein extract was washed with 2 M urea in 100 mM Tris-HCl and then with 50 mM ammonium bicarbonate for digestion with endoproteinase LysC (1:10 w:w, 37°C, o/n) and then for trypsin digestion (1:10 w:w, 37°C, 8h, Promega). After digestion, peptide mix was acidified with formic acid and desalted with a MicroSpin C18 column (The Nest Group, Inc) prior to LC-MS/MS analysis.

Chromatographic and MS data acquisition

Samples were analyzed using an LTQ-Orbitrap XL mass spectrometer (Thermo Fisher Scientific, San Jose, CA, USA) coupled to an EASY-nLC (Thermo Fisher Scientific (Proxeon), Odense, Denmark). Peptides were loaded onto the 2-cm Nano Trap column with an inner diameter of 100 μm packed with C18 particles of 5 μm particle size (Thermo Fisher Scientific) and were separated by reversed-phase chromatography using a 12-cm column with an inner diameter of 75 μm, packed with 3 μm C18 particles (Nikkyo Technos Co., Ltd. Japan). Chromatographic gradients started at 97% buffer A and 3% buffer B with a flow rate of 300 nl/min for 4 minutes and gradually increased to 5% buffer B and 95% buffer A in 1 min and to 65% buffer A and 35% buffer B in 120 min. After each analysis, the column was washed for 10 min with 10% buffer A (0.1% formic acid in water) and 90% buffer B (0.1% formic acid in acetonitrile). The mass spectrometer was operated in positive ionization mode with nanospray voltage set at 2 kV and source temperature at 200°C. The acquisition was performed in data-dependent acquisition (DDA) mode and full MS scans with 1 micro scans at resolution of 60,000 were used over a mass range of m/z 350-1500 with detection in the Orbitrap mass analyzer. Auto gain control (AGC) was set to 1E5, dynamic exclusion (90 s) and charge state filtering disqualifying singly charged peptides was activated. In each cycle of DDA analysis, following each survey scan, the top ten most intense ions with multiple charged ions above a threshold ion count of 5,000 were selected for fragmentation. Fragment ion spectra were produced via collision-induced dissociation (CID) at normalized collision energy of 35% and they were acquired in the ion trap mass analyzer. AGC was set to 1E4, isolation window of 2.0 m/z, activation time of 30 ms and maximum injection time of 100 ms was used. All data were acquired with Xcalibur software v2.1.

MS data analysis

Acquired spectra were analyzed using the Proteome Discoverer software suite (v2.0, Thermo Fisher Scientific) and the Mascot search engine (v2.6, Matrix Science) (Perkins et al., 1999). The data were searched against a Swiss-Prot *Schizosaccharomyces pombe* reference proteome database (as in June 2019) plus a list of common contaminants and all the corresponding decoy entries (Beer et al., 2017). For peptide identification a precursor ion mass tolerance of 7 ppm was used for MS1 level, trypsin was chosen as enzyme and up to three missed cleavages were allowed. The fragment ion mass tolerance was set to 0.5 Da for MS2 spectra. Oxidation of methionine and N-terminal protein acetylation were used as variable modifications whereas carbamidomethylation on cysteines was set as a fixed modification. Peptide quantification data were retrieved from the ''Precursor ion area detector'' node from Proteome Discoverer (v2.0) using 2 ppm mass tolerance for the peptide extracted ion current (XIC). The obtained values were used to calculate protein fold-changes. p values were generated using unpaired t test and their corresponding adjusted p values (q-values) by False Discovery Rate (FDR). A Venn diagram of insoluble proteins at different conditions was created using an online tool of the Bioinformatics and Evolutionary Genomics website (Ghent University); only proteins present in 2 out 3 replicates (1032, 1135, 1228 at 30°C, 37°C and 42°C respectively) were included in this analysis. Volcano plots including $\log_2$ fold changes in protein abundance and - $\log_{10}$ q-values were generated using R software and ggplot2 package. Gene Ontology (GO) term enrichment was obtained using Quick Little Tool (QuiLT, Pombase) for cellular component GO terms and BINGO tool [Cytoscape, (Shannon et al., 2003)] for molecular function and biological process GO terms. Hypergeometric test, Benjamini and Hochberg FDR correction and a significance level of 0,05 were selected in the BINGO analysis. GO terms were visualized using Excel.

QUANTIFICATION AND STATISTICAL ANALYSIS

Quantification of Western Blots was performed using Image Studio Lite (LICOR Biosciences). Unless otherwise stated, all experiments were performed at least three times and representative experiments were shown. In the bar graphs, bar heights represent the mean values and the error bars SD or SEM. Statistical details of MS experiments are included in the Method Details section.

DATA AND CODE AVAILABILITY

The raw proteomics data have been deposited to the PRIDE (Vizcaíno et al., 2016) repository with the dataset identifier PXD014400. All images included in the main and supplemental figures are available as Mendeley dataset (https://doi.org/10.17632/fxxynrt6hj.1).